

Nonlinear acoustoelectric interactions in GaAs/LiNbO₃ structures

Cite as: Appl. Phys. Lett. **75**, 965 (1999); <https://doi.org/10.1063/1.124568>

Submitted: 07 May 1999 • Accepted: 21 June 1999 • Published Online: 10 August 1999

M. Rotter, A. Wixforth, A. O. Govorov, et al.



View Online



Export Citation

ARTICLES YOU MAY BE INTERESTED IN

[Giant acoustoelectric effect in GaAs/LiNbO₃ hybrids](#)

Applied Physics Letters **73**, 2128 (1998); <https://doi.org/10.1063/1.122400>

[Linear and Nonlinear Attenuation of Acoustic Surface Waves in a Piezoelectric Coated with a Semiconducting Film](#)

Journal of Applied Physics **41**, 454 (1970); <https://doi.org/10.1063/1.1658696>

[Acoustically induced current flow in graphene](#)

Applied Physics Letters **100**, 133105 (2012); <https://doi.org/10.1063/1.3697403>

 QBLOX



1 qubit

Shorten Setup Time

Auto-Calibration
More Qubits

Fully-integrated
Quantum Control Stacks
Ultrastable DC to 18.5 GHz
Synchronized <<1 ns
Ultralow noise



100s qubits

[visit our website >](#)

Nonlinear acoustoelectric interactions in GaAs/LiNbO₃ structures

M. Rotter and A. Wixforth

Sektion Physik der LMU and CeNS, Geschw.-Scholl-Platz 1, 80539 München, Germany

A. O. Govorov

Institute of Semiconductor Physics, 630090 Novosibirsk, Russia

W. Ruile, D. Bernklau, and H. Riechert

Siemens AG, Corporate Technology, 81730 München, Germany

(Received 7 May 1999; accepted for publication 21 June 1999)

Surface acoustic waves accompanied by very large piezoelectric fields can be created in a semiconductor/piezoelectric hybrid system. Such intense waves interact with the mobile carries in semiconductor quantum well structures in a manner being strongly governed by nonlinear effects. At high sound intensities, a formerly homogeneous two-dimensional electron system breaks up into well confined stripes surfing the wave. As a result, we observe a strong reduction of electronic sound attenuation. On the other hand, large momentum transfer between the electron system and the wave results in nonlinear acoustoelectric effects and acoustoelectric amplification. We describe our experimental findings in terms of a generalized theory of the acoustoelectric effect and discuss the importance for possible device applications. © 1999 American Institute of Physics.

[S0003-6951(99)02533-4]

Over the last decade, interaction phenomena between surface acoustic waves (SAW) and a two-dimensional electron system (2DES) have attracted much interest. Rayleigh wave modes on monolithic GaAs/AlGaAs heterostructures were used to examine the magnetoconductivity properties of the electron system in the integer quantum hall regime¹ and gave the most striking evidence for the composite fermion picture of the fractional quantum hall effect.² The piezoelectric fields accompanying the waves were also employed to convey single electrons through a quantum point contact.³ For all these experiments, however, the SAW were excited and propagating on the relatively weak piezoelectric semiconductor substrate itself, in most cases GaAs. This implies a relatively weak coupling between mobile carriers in the semiconductor and the SAW, being quantified in a small electromechanical coupling coefficient K .² However, on strong piezoelectric substrates like LiNbO₃, this coupling coefficient is two orders of magnitude larger. Thus, hybridization of a LiNbO₃ substrate and a thin GaAs-based quantum well system provides a very large coupling coefficient⁴ and we proceed into a new regime of nonlinear interaction between SAW and 2DES, manifested in a large momentum transfer from the SAW to the electrons and vice versa. We achieve the hybridization of the LiNbO₃ crystal and the thin layers of the semiconductor heterostructure with a thickness of 0.5 μm by employing the epitaxial lift-off technique (ELO).⁵ In this process, we remove the semiconductor film from its original GaAs substrate and transfer it onto a LiNbO₃ SAW delay line.^{4,6} The 2DES resides in a 12 nm In_{0.2}Ga_{0.8}As quantum well, where the distance between the electron system and the hybrid interface is only 32 nm. A thin metal field effect electrode on top of the ELO film acts as a gate to change the carrier density n_s and the sheet conductivity σ of the well. Interdigital transducers (IDT) on the LiNbO₃ serve as emitter and detector for the SAW (see Fig. 3), operating at an rf frequency of $f = 340$ MHz. This hybrid

structure allows for detailed investigations on the interaction between SAW and 2DES at very large sound amplitudes and strong coupling.

When the SAW propagates through the semiconductor film containing the electron system, the accompanying piezoelectric fields E_{SAW} generate dissipative currents, resulting in an attenuation of the wave, $\Gamma = \langle j E_{\text{SAW}} \rangle / I$, where I denotes the SAW intensity and the brackets denote the averaging over one wave period. Neglecting carrier diffusion, the local dissipative current density j is given by $j = ne\mu(E_{\text{SAW}} + E_{\text{2DES}})$, where E_{2DES} is the electric field induced by the modulated electron system; n is the local electron density, and μ is the mobility of the 2DES. For low SAW intensity the modulation of the carrier concentration is also very small and the attenuation can be evaluated in a linear approach, leading to the following equation:^{7,1}

$$\Gamma = K_H^2 \frac{\pi}{\lambda} \frac{\sigma / \gamma \sigma_m}{1 + (\sigma / \gamma \sigma_m)^2}. \quad (1)$$

Here, K_H^2 denotes the electromechanical coupling coefficient of the hybrid,⁶ and λ is the sound wavelength. An electron drift parameter γ , which will be discussed in detail below, is set to $\gamma = 1$ at this time. At a certain conductivity σ_m the electron system absorbs a significant amount of the SAW power. This is displayed in the inset of Fig. 1, where we plot the measured attenuation of the SAW as a function of the gate voltage V_g between gate and 2DES for various SAW powers at room temperature. Zero gate bias corresponds to a high sheet conductivity; a large potential difference (e.g., $V_g = -10$ V) leads to a depletion of the quantum well. First, let us consider the case for small SAW intensity I ($P = 0.13$ mW): Around $V_g = -8$ V energy is transferred from the SAW to the 2DES resulting in an attenuation of the SAW, being well described by Eq. (1). For high SAW intensity, however, the 2DES is strongly modulated resulting in a

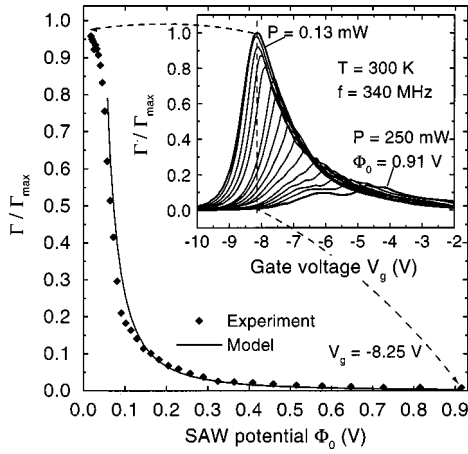


FIG. 1. Normalized SAW attenuation Γ/Γ_{\max} at constant gate voltage $V_g = -8.25$ V as a function of the SAW potential amplitude Φ_0 . The inset shows Γ/Γ_{\max} as a function of the gate voltage V_g with the SAW potential as parameter. The theoretical result of our model according to Eq. (2) is also shown for comparison.

strong reduction of the SAW attenuation Γ . This phenomenon can be explained in terms of a nonlinear theory⁸ for the 2D case. In this model we calculate the local carrier concentration n in the SAW potential. We find, that for high SAW intensity and small carrier density n_s the electrons are completely trapped in the SAW potential. In this case, the carrier distribution n can be calculated analytically. The electrons are forming stripes moving at the speed of sound⁸ and the absorbed SAW energy $\langle jE_{\text{SAW}} \rangle$ saturates. In this regime, the attenuation Γ is reduced and is analytically given by

$$\Gamma = \frac{\langle jE_{\text{SAW}} \rangle}{I} = \frac{en_s v^2}{\mu I} = \frac{en_s v^2}{\mu a \Phi_0^2}, \quad (2)$$

where v is the SAW phase velocity and a denotes a constant correlating the SAW intensity and the square of the SAW potential amplitude Φ_0^2 . In Fig. 1 we show this behavior experimentally, displaying the attenuation as a function of the SAW potential for fixed gate voltage $V_g = -8.25$ V, corresponding to a fixed carrier density of about $n_s = 5.6 \times 10^9 \text{ cm}^{-2}$. This carrier concentration being determined by $\sigma_m = 3.6 \times 10^{-6} \Omega^{-1}$ and $\mu \approx 4000 \text{ cm}^2/\text{Vs}$ is sufficiently low to satisfy the criteria for Eq. (2) at large SAW potential, where the electrons have to be totally trapped. We also plot the calculated attenuation according to Eq. (2). Theory and experiment are in excellent agreement. The change of conductivity also produces a change in SAW velocity.^{4,6} Since the total value of the velocity change is not affected by the strong modulation of n_s ,⁸ the effect of the reduced SAW attenuation is very interesting for SAW devices where the SAW velocity could be tuned by an applied gate bias.

The transfer of power from the SAW to the 2DES is also related to momentum transfer from the acoustic wave to the electron system. The resulting acoustoelectric current j_{ae} was studied before for small SAW power in various experiments.^{9,6} For a three-dimensional (3D) bulk system, the connection between j_{ae} and Γ had been described before by Weinreich.^{10,11} For a two-dimensional electron system, this acoustoelectric current can be also calculated in a linear small signal model.¹² Here, we develop a nonlinear approach for the two-dimensional case, and describe the dynamics in

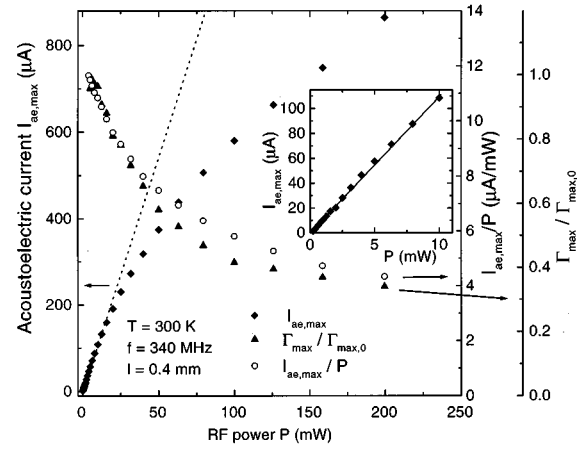


FIG. 2. Maximum of the acoustoelectric current $I_{ae,\max}$ and maximum of the SAW attenuation $\Gamma_{\max}/\Gamma_{\max,0}$ as a function of the applied rf power P . For small P , the acoustoelectric current exhibits a linear behavior, which is shown in the inset. The linear regression from the inset is also displayed in the main figure, revealing the strong deviation from linearity. Also shown is the ratio $I_{ae,\max}/P$ (open symbols) to demonstrate the predicted universal proportionality between $I\Gamma$ and the acoustoelectric current j_{ae} . l denotes the length of the ELO film.

an intense SAW field by a nonlocal and nonlinear equation.⁸ We assume that Γ is small compared to $1/\lambda$, so that the electron density n can be assumed to be periodically modulated. The acoustoelectric current is then given by the averaged current

$$j_{ae} = \langle j(x,t) \rangle = e\mu \langle n(E_{\text{SAW}} + E_{2\text{DES}}) \rangle = e\mu \langle \langle nE_{\text{SAW}} \rangle + \langle nE_{2\text{DES}} \rangle \rangle. \quad (3)$$

$E_{2\text{DES}}$ is the electric field induced by the 2DES. $\langle jE_{2\text{DES}} \rangle$ is zero, because of the conservation of energy and therefore leads to

$$0 = \langle jE_{2\text{DES}} \rangle = j_0 \langle E_{2\text{DES}} \rangle - e v \langle nE_{2\text{DES}} \rangle = -e v \langle nE_{2\text{DES}} \rangle. \quad (4)$$

The current density j_0 results as a constant when integrating the continuity equation.⁸ The averaged values $\langle E_{\text{SAW}} \rangle$ and $\langle E_{2\text{DES}} \rangle$ vanish due to the periodicity of the problem and hence also $\langle nE_{2\text{DES}} \rangle$ vanishes [Eq. (4)]. The first term in Eq. (3) can be expressed by the attenuation Γ , since the SAW absorption is given as $I\Gamma = \langle jE_{\text{SAW}} \rangle = j_0 \langle E_{\text{SAW}} \rangle - e v \langle nE_{\text{SAW}} \rangle = -e v \langle nE_{\text{SAW}} \rangle$. This gives us a final expression for the acoustoelectric current

$$j_{ae} = -\frac{\mu I \Gamma}{v}, \quad (5)$$

being independent of the SAW potential modulation. This expression resembles the Weinreich relation¹⁰ for bulk waves and 3D electron systems. No matter, how strong electrons are bunched in the moving SAW potentials, the relation between the acoustoelectric current, the SAW intensity and the attenuation remains the same.

Experimentally, we observe just this behavior when measuring the acoustoelectric current in a geometry similar to the sample geometry similar to the one described below. For various different SAW intensities, the acoustoelectric current and the attenuation were recorded as a function of the gate bias V_g . In Fig. 2 we show the measured maximum

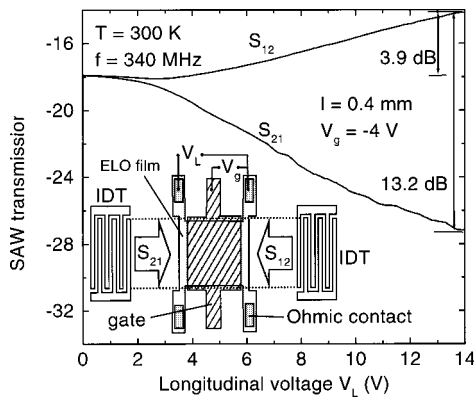


FIG. 3. Bidirectional SAW transmission S_{12} and S_{21} as a function of a longitudinal voltage V_L applied to the ohmic contacts. Depending on the direction of the SAW, either field-induced amplification or attenuation can be observed, resulting in a nonreciprocal acoustoelectric device. The inset shows the sample geometry with the interdigital transducers (IDT) and the ELO film.

value of the acoustoelectric current, $I_{ae,max}$, together with the maximum of the attenuation as a function of the rf power P applied to the emitting transducer. For small P , we observe a linear behavior of the acoustoelectric current as a function of P , which is shown in the inset. However, for high P , the acoustoelectric current $I_{ae,max}$ does not follow this linear regression, and increases in a sublinear fashion. At the same time, the attenuation is strongly reduced with increasing SAW power. It should be noted, that the reduction is not as large as in Fig. 1, because we measure the absolute maximum of the attenuation instead of the attenuation at a given gate bias (Fig. 1). To correlate these experimental findings with our model, we also show the ratio $I_{ae,max}/P$ being proportional to $j_{ae,max}/l$. Figure 2 displays clearly, that this ratio $I_{ae,max}/P$ is proportional to the attenuation Γ as predicted by Eq. (5). The observed nonlinearity in the acoustoelectric current can thus be very well understood in terms of our model. At this point, we wish to point out the remarkable amplitude of the observed currents in our hybrid system. Because of the large hybrid coupling coefficient, it extends up to $I_{ae,max} = 0.7$ mA.

Momentum transfer from the SAW to the 2DES is only one part of the interaction between surface acoustic waves and an electron system. We can also transfer energy from an electron flow in the 2DES to the SAW. This effect is known as ‘‘acoustoelectric amplification.’’⁷ However, in monolithic GaAs heterostructures the effect is very small,¹³ because of the small coupling coefficient. We use again the sample geometry as shown in Fig. 3. A longitudinal dc voltage V_L is now applied to the ohmic contacts in order to create an external electric field E_L and an electron drift current. As soon as the electron drift velocity v_d exceeds the sound velocity v , energy is transferred to the SAW. Quantitatively, this is already described by Eq. (1), employing the electron drift parameter $\gamma = 1 + \mu E_L/v = 1 + v_d/v$. Equation (1) also reveals, that a large amplification can only be achieved, if the sheet conductivity σ is sufficiently low. Therefore a gate bias V_g is applied to reduce σ . Figure 3 displays the measured SAW transmission S_{12} and S_{21} for both directions of SAW propagation. If the SAW is launched from the transducer on the right hand side (S_{12}), the wave is amplified with increas-

ing E_L . Amplification of 3.9 dB is achieved in this geometry. Theoretically, from Eq. (1) and the sample parameters used, one would expect a maximum amplification of 7.9 dB but one can show that the observed reduction is caused by pinch-off effects that create a conductivity gradient along the channel. We hope to reduce these spurious effects by a better suited sample design in the near future.

If the wave is launched from the other transducer, the SAW is propagating in the opposite direction than the electrons and therefore the wave is attenuated with increasing longitudinal voltage V_L . Employing these effects, a new nonreciprocal SAW filter could be realized. In one direction, the transmitted signal is amplified, in the other direction, it is attenuated. Using optimized and matched unidirectional transducer structures, the insertion loss of the device for $V_L = 0$ could be reduced to about 3–4 dB so that a net amplification of an rf signal could be achieved.

In summary, we have demonstrated several acoustoelectric effects in the LiNbO₃/GaAs layered system on which large amplitude SAW can be coupled to mobile carriers in a quantum well. We find that at large SAW amplitudes the electron density can be modulated very strongly, eventually breaking up into stripes. This leads to a significant reduction of the SAW attenuation. In a nonlinear theory, we can describe this phenomenon quantitatively. Because of the high coupling coefficient, the SAW induce large acoustoelectric currents which exhibit a strong nonlinear behavior as a function of the amplitude of the SAW potential. We present a generalized theoretical description of the acoustoelectric effect in 2D which is in excellent agreement with our experimental observations. Finally, we demonstrate acoustic amplification in our hybrid system which makes nonreciprocal SAW filters with monolithically integrated signal amplification feasible.

The authors gratefully acknowledge the technical assistance of S. Manus, T. Ostertag, and S. Berek and many valuable discussions with A. V. Kalameitsev and J. P. Kotthaus. M.R. acknowledges financial support by Siemens and DFG (Wi 1091/4-2).

- ¹A. Wixforth, J. P. Kotthaus, and G. Weimann, Phys. Rev. B **40**, 7874 (1989).
- ²R. L. Willet, R. R. Ruel, K. W. West, and L. N. Pfeiffer, Phys. Rev. Lett. **71**, 3846 (1993).
- ³V. I. Talyanskii, J. M. Shilton, M. Pepper, C. G. Smith, C. J. B. Ford, E. H. Linfield, D. A. Ritchie, and G. A. C. Jones, Phys. Rev. B **56**, 15180 (1997).
- ⁴M. Rotter, C. Rocke, S. Böhm, A. Lorke, A. Wixforth, W. Ruile, and L. Korte, Appl. Phys. Lett. **70**, 2097 (1997).
- ⁵E. Yablouovich, D. M. Hwang, T. J. Gmitter, L. T. Florez, and J. P. Harbison, Appl. Phys. Lett. **56**, 2419 (1990).
- ⁶M. Rotter, A. Wixforth, W. Ruile, D. Bernklau, and H. Riechert, Appl. Phys. Lett. **73**, 2128 (1998).
- ⁷D. L. White, J. Appl. Phys. **33**, 2547 (1962).
- ⁸M. Rotter, A. V. Kalameitsev, A. O. Govorov, W. Ruile, and A. Wixforth, Phys. Rev. Lett. **82**, 2171 (1999).
- ⁹A. Esslinger, R. W. Winkler, C. Rocke, A. Wixforth, J. P. Kotthaus, H. Nickel, W. Schlapp, and R. Lösch, Surf. Sci. **305**, 83 (1994).
- ¹⁰V. I. Fal’ko, S. V. Meshkov, and S. V. Iordanskii, Phys. Rev. B **47**, 9910 (1993).
- ¹¹G. Weinreich, Phys. Rev. **107**, 317 (1957).
- ¹²Yu. V. Gulyaev, Sov. Phys. Solid State **12**, 328 (1970).
- ¹³T. P. Cameron and W. D. Hunt, Proceedings of IEEE Ultrasonic Symposium 1995, 349, IEEE Cat. No. 95CH35844, New York (unpublished).